IOVS Papers in Press. Published on March 12, 2015 as Manuscript iovs.15-16520

TITLE: Lack of interphotoreceptor retinoid binding protein, caused by homozygous mutation of *RBP3*, is associated with high myopia and retinal dystrophy.

AUTHORS: Gavin Arno PhD [1, 2]; Sarah Hull MA, FRCOphth [1, 2]; Anthony G Robson MSc, PhD [1, 2]; Graham E Holder MSc, PhD [1, 2]; Michael E Cheetham PhD [1]; Andrew R Webster MD(res), FRCOphth [1, 2]; Vincent Plagnol PhD [3]; Anthony T Moore MA, FRCOphth [1, 2, 4,5]

1. UCL Institute of Ophthalmology, London, United Kingdom.
2. Moorfields Eye Hospital, London, United Kingdom.
3. University College London Genetics Institute, London, United Kingdom
4. Ophthalmology Department, Great Ormond Street Hospital for Children NHS Trust, London, United Kingdom.
5. Department of Ophthalmology University of California San Francisco

Financial Disclosure: The authors have no proprietary or commercial interest in any materials discussed in this article

Funding: The National Institute for Health Research (UK) and Biomedical Research Centre at Moorfields Eye Hospital and the UCL Institute of Ophthalmology, The Foundation Fighting Blindness (USA), Fight For Sight, Moorfields Eye Hospital Special Trustees, Rosetrees Trust

Conflict of Interest: No conflicting relationship exists for any author

Running head: Nonsense mutations of *RBP3* and retinal dystrophy

Address for reprints: Prof Moore, Inherited Eye Diseases, UCL Institute of Ophthalmology, 11-43 Bath St, London, EC1V 9EL

Copyright 2015 by The Association for Research in Vision and Ophthalmology, Inc.

Abstract

Purpose: To present a detailed clinical and molecular study of four patients from two consanguineous families with a similar childhood-onset retinal dystrophy resulting from novel homozygous nonsense mutations in *RBP3.*

Methods: Four children with mutations in *RBP3* encoding interphotoreceptor binding protein (IRBP) were ascertained by whole exome sequencing and subsequent direct Sanger sequencing. Detailed phenotyping was performed including full clinical evaluation, electroretinography, fundus photography, fundus autofluorescence (FAF) imaging and spectral domain optical coherence tomography (OCT).

Main Outcome Measures: Results of ophthalmic examination, whole exome sequence analysis and Sanger sequence analysis.

Results: Two novel homozygous nonsense mutations (c.1530T>A ; p.Y510* and c.3454G>T ; p.E1152*) in *RBP3* were identified in four patients from two families. All four patients had a similar, unusual retinal dystrophy characterized by childhood onset high myopia, generalized rod and cone dysfunction and an unremarkable fundus appearance. FAF imaging showed multiple paracentral foci of low autofluorescence in one patient and patchy increased FAF in the region of the vascular arcades in another. The OCT showed loss of outer retinal bands over peripheral macular areas in all 4 cases.

Conclusions: This report is the first to describe the retinal dystrophy in children caused by homozygous nonsense *RBP3* mutations highlighting the requirement for IRBP in normal eye development and visual function. Longitudinal study will reveal if the four children reported here will progress to a more typical retinitis pigmentosa phenotype previously described in adults with *RBP3* mutations. *RBP3* related disease should be considered in children with high myopia and retinal dystrophy, particularly when there are no significant fundus changes.

Introduction

RBP3 (MIM *180290) encodes the Inter-photoreceptor retinoid binding protein (IRBP), a 140-145kDa glycoprotein exclusively expressed by photoreceptors and the pineal gland. Expression of IRBP by rod and cone photoreceptors is reliant on trans-activation by the retina and pineal gland specific transcription factor Cone-Rod Homeobox (CRX)[1,2]. It is the most abundant protein found in the inter-photoreceptor matrix (IPM), the extracellular space between the photoreceptor outer segments and the retinal pigment epithelium (RPE)[3–5]. *RBP3* comprises four contiguous homologous repeats encoding retinoid binding modules of approximately 300 amino acid residues. These modules show structural homology to the C-terminal processing protease (CTPase) and crotonase superfamily that all use a ββα-spiral fold to bind hydrophobic ligands[6]. The four modules together in IRBP may bind a single retinoid molecule[7].

Early, in vitro studies showed that IRBP could facilitate the release of all-trans-retinol (ROL) by photoreceptor outer-segments and delivery to the RPE, and in turn, the release of 11-cis-retinal (RAL) by RPE cells[8,9]. This led to the suggestion that IRBP is involved with the transport of retinoids across the IPM including the maintenance of the isomeric state of retinoids during passage across the matrix[10–12]; however, the role of IRBP in the visual cycle that replenishes 11-cis-RAL is controversial. Initial investigation of the *Irbp*-/- knockout (KO) mouse showed that IRBP was not essential for recycling of the chromophore 11-cis-RAL[13]. In the classical visual cycle, all-trans-ROL is

removed from the outer segments to be isomerised back to 11-cis-RAL by RPE65 in the RPE cells. Cones may use an additional process whereby all-trans-ROL is transported to the Müller cells where it is converted to 11-cis-ROL and transported back to the cones which can oxidise it to 11-cis-RAL(reviewed in:[14]). Specific investigation of the role of IRBP in cone function showed that IRBP deletion altered the balance of retinoids in the retina and also affected normal cone function, which could be rescued with 9-cis-RAL[15,16]. Furthermore, the ability of IRBP to protect 11-*cis*-ROL from isomerization in light may allow cones to produce 11-*cis*-RAL under photopic conditions and enable continuous cone function in constant light[17]. In contrast, investigation of the *irbp* KO on a rod transducin KO background, where only the cones respond to light, revealed no major defects in cone function, although the kinetics of mouse M/L-cone photoresponses were slowed[18]. Furthermore, under conditions where RPE65 activity is high (e.g. the Leu450 variant in mouse) then IRBP is needed to maintain maximal rod dark adaptation[18], suggesting IRBP might affect both rod and cone function dependent on conditions.

The *Irbp-/-* KO mouse shows abnormalities of photoreceptor morphology as early as 11 days postnatally, and significantly reduced photoreceptor survival and electroretinogram (ERG) responses by one month of age, with slow progression thereafter [19,20]. These findings suggested *RBP3* to be a candidate gene for human retinal disease. In 2009, den Hollander and colleagues identified a shared homozygous region of chromosome 10 in four adult siblings from a consanguineous Italian family with autosomal recessive

retinitis pigmentosa (arRP)[21]. A homozygous missense change in the fourth retinol binding module of *RBP3* (c.3238G>A, p.D1080N) was identified by Sanger sequencing. Since that report no further patients have been documented with mutations in *RBP3.*

The present report describes the phenotype in 4 young patients with *RBP3* mutations, and identifies 2 novel disease-causing mutations.

Methods

The study protocol adhered to the tenets of the Declaration of Helsinki and received approval from the local ethics committee. Written, informed consent was obtained from all participants or in the case of minors, their parents prior to their inclusion in this study.

Each patient with an *RBP3* mutation underwent a full clinical examination including visual acuity and dilated fundus examination. Retinal fundus imaging was obtained by conventional 30 degree fundus color photographs (Topcon Great Britain Ltd, Berkshire, UK), 30 and 55 degree fundus autofluorescence (FAF) imaging, and spectral domain optical coherence tomography (OCT) scans (Spectralis, Heidelberg Engineering Ltd, Heidelberg, Germany). Full field electroretinography (ERG) and pattern electroretinography (PERG) were performed using gold foil electrodes to incorporate the International Society for Clinical Electrophysiology of Vision (ISCEV) standards[22,23].

Molecular genetics

The subjects described here were part of a larger whole exome sequencing (WES) study of patients with childhood onset retinal dystrophies. Eighty probands and family members were recruited to the study. Patients were included based on at least one of the following criteria (1) unknown molecular diagnosis following previous investigations, (2) known parental consanguinity (3) unusual phenotype with no known molecular association, (4) >1 affected family member. Patient 1 from a Kurdish family from Turkey was selected for WES based on parental consanguinity, unusual clinical phenotype and the presence of a similarly affected sibling. DNA samples were isolated from peripheral blood lymphocytes using the Puregene DNA extraction kit (Gentra Puregene Blood Extraction Kit, QIAGEN, Manchester, UK). Exon capture was performed using the SureSelectXT Human All Exon V5 kit (Agilent, CA, USA). Paired-end sequencing was carried out using a Hiseq2500 high throughput sequencer (Illumina, CA, USA) at AROS Applied Biotechnology (Aarhus, Denmark).

The raw FASTQ output files comprising FASTA formatted text based sequence and quality data for each read were aligned to the Genome Reference Consortium human genome build 37 (GRCh37) using Novoalign version 2.08.03 (Novocraft technologies, Malaysia). Duplicate reads were flagged using Markduplicates (Picard Tools, Broad institute, Cambridge, MA, USA, http://broadinstitute.github.io/picard). Sequence variants were called using the Haplotype Caller module of the Genome Analysis ToolKit (GATK,

Broad institute, Cambridge, MA, USA, https://www.broadinstitute.org/gatk) version 3.3-0 creating a genomic variant call file (gVCF) formatted file for each patient sample. The individual gVCF files discussed in this study, in combination with gVCF files of ~ 3,000 clinical exomes (UCL-exomes consortium), were combined into merged VCF files for each chromosome containing on average 100 samples each. The final variant calling was performed using the GenotypeGVCFs module (GATK, Broad institute, Cambridge, MA, USA https://www.broadinstitute.org/gatk) jointly for all samples (cases and controls). Variant quality scores were then re-calibrated according to GATK best practices separately for insertion/deletions (Indels) and Single nucleotide variants (SNVs). Resulting variants were annotated using the ANNOVAR (http://www.openbioinformatics.org/annovar/) tool based on Ensembl (http://www.ensembl.org) gene and transcript definitions. Candidate variants were filtered based on function (non synonymous, presumed loss-of-function or splicing, defined as intronic sites within 5 bp of an exon-intron junction) and minor allele frequency (< 0.5% minor allele frequency in our internal control group, as well as the NHLBI GO Exome Sequencing Project dataset).

Subsequently, 7 patients with a similar clinical phenotype of high myopia and retinal dystrophy were ascertained and screened for mutations by direct Sanger sequencing of the coding exons of *RBP3* including the intron/exon boundaries (PCR primers and conditions available on request).

Mutation nomenclature was assigned in accordance with GenBank Accession number NM_002900.2 with nucleotide position 1 corresponding to the A of the ATG initiation codon. Variants were identified as novel if not previously reported in the literature and if absent from all any online variant database including:

-Database of Single Nucleotide Polymorphisms (dbSNP). Bethesda (MD): National Center for Biotechnology Information, National Library of Medicine. (dbSNP Build 142) Available from: http://www.ncbi.nlm.nih.gov/SNP/

-NHLBI GO Exome Sequencing Project (ESP), Seattle, WA (URL: http://evs.gs.washington.edu/EVS/) [accessed September 2014]

-1,000 genomes project[24]

-Exome aggregation Consortium (ExAC) Cambridge, MA (URL: http://exac.broadinstitute.org) [accessed October 2014].

Results

Four patients, age 8-14 years, from 2 families, were identified with retinal dystrophy due to biallelic mutation of *RBP3* (Figure 1). Full clinical data are summarized in table 1. Visual acuities were measured in logMAR units and approximate Snellen values are additionally given below.

Family GC17452

Two siblings from this family were noted to have strabismus and reduced vision in infancy. The parents were first cousins but there was no family

history of eye problems. They were referred to their local unit where they were found to be highly myopic and spectacles were prescribed. Visual acuity remained poor despite refractive correction.

The older sibling (Patient 1) was first seen at Moorfields Eye Hospital (MEH) at age 5 years. His parents had, by then, noted poor night vision. His best corrected visual acuity was 0.550 logMAR (Snellen 20/80) in right eye and 0.575 (Snellen 20/80) in the left. Fundus examination showed a tessellated appearance but was otherwise unremarkable. The OCT showed relative preservation over the central macula with retinal thinning and loss of the inner segment ellipsoid band (ISe) over eccentric macular areas. The electrophysiology was in keeping with a cone-rod dystrophy. Full-field ERGs, performed at the age of 10 years, revealed delay and amplitude reduction in ERG cone responses and less marked dysfunction in the rod system; the undetectable pattern ERG showed severe macular involvement. (Figure 2).

The younger sibling (Patient 2) was first seen at MEH age 4years. She was also myopic and reported to have poor night vision. The best corrected visual acuity was 0.475 logMAR (20/63 Snellen) right and 0.650 (Snellen 20/100) left. Examination revealed a tessellated fundus appearance. There was patchy increased FAF in the region of the vascular arcades (Figure 3). The OCT showed loss of the ISe over peripheral macular areas. Full-field ERGs, performed at the age of 9 years, revealed a similar pattern of abnormality to her male sibling but with less marked rod-system involvement (Figure 2).

Family GC19774

Both affected brothers in this family were noted in infancy to sit near to the television and hold toys very close. Neither brother appeared to have problems with night vision. The parents were first cousins but there was no family history of eye problems. Clinical evaluation revealed high myopia but vision could not be improved to normal with refraction.

The older sibling (Patient 3) was first seen age 2 years. There was a small exophoria and bilateral myopia. Fundus examination revealed myopic discs and a tessellated fundus but was otherwise unremarkable. At age 4 years visual acuity was 0.35 logMAR (Snellen 20/50) right and 0.325 logMAR (Snellen 20/40). The OCT showed loss of the ISe over peripheral macular areas. Full field ERG (Figure 2) showed evidence of rod and cone dysfunction with the rod system probably more affected; the PERG was normal indicating macular sparing. Repeat testing at aged 13 (not shown) demonstrated marked deterioration in cone function, with less marked rod system deterioration. The phenotype had developed into a cone-rod rather than rod-cone pattern of abnormality. Pattern ERG was undetectable consistent with severe worsening of macular function. At the last clinic visit age 14 years best corrected visual acuity was 0.12 logMAR (Snellen 20/25) and 0.02 logMAR (Snellen 20/20)

The younger sibling (Patient 4) was first seen age 2 years. He had a small left esotropia. Fundus examination was unremarkable. His visual acuity at age 5

years was 0.45 logMAR (Snellen 20/63) right and 0.425 logMAR (Snellen 20/50) left. The OCT showed loss of the ISe over peripheral macular areas (Figure 3). FAF showed multiple paracentral foci of reduced signal with a normal central macula. Electrophysiological testing at age 7 years (Figure 2) showed ERG evidence of rod and cone dysfunction, with the rod-system probably more affected; the PERG showed relative macular sparing.

Molecular findings

WES analysis of patient 2 revealed 25,799 exonic or presumed splice altering (within 5 bp of exon-intron junctions) variant calls after quality filtering (Table 2). Of these, 623 had an allele frequency of <0.1% in the NHLBI ESP database. Of these 623 variants, 27 were homozygous variants, of which two were predicted to be loss of function (LOF). Of these two, a nonsense variant in the final exon of *RBP3* – c.3454G>T ; p.E1152*, was identified as the likely causative variant due to the previous association of *RBP3* mutations with a retinal dystrophy. The homozygous variant call was subsequently confirmed in the both affected siblings by Sanger sequencing; both parents were heterozygous.

Seven unrelated patients with a similar retinal phenotype and high myopia underwent Sanger sequencing of *RBP3* and one further homozygous nonsense mutation (c.1530T>A ; p.Y510*) was identified in exon 1 of *RBP3* in two affected siblings of family GC19774. Parental DNA was unavailable for screening.

Neither of these nonsense mutations were identified in our control set of 2,571 samples (UCL-exomes), or any online database. The ExAC database includes exome sequencing variants from 61,486 individuals and contains 38 heterozygous alleles of 20 predicted LOF variants in *RBP3* comprising 12 frameshift and 8 nonsense variants. Nineteen of these variants were found in ≤4 alleles, one was found in 10/16628 (0.06% minor allele frequency) alleles of South Asian origin, these might represent carriers of rare retinal dystrophy alleles.

Discussion

This report describes a novel phenotype in patients with retinal dystrophy consequent upon mutation in *RBP3.* The disorder involves both rod and cone systems. Some patients have marked central retinal involvement, and can be described as having a cone-rod pattern of dysfunction; others have a rod-cone pattern with macular sparing early in the course of the disorder which, in one patient, subsequently showed clear cone>rod dysfunction. Two novel mutations are reported.

The first report of *RBP3* mutation associated with retinal disease appeared in 2009[21], describing autosomal recessive RP in a consanguineous Italian family. Affected individuals had onset of central vision loss in adult life with or without night-blindness; the onset of symptoms ranged from 32 to 60 years of age. The clinical findings were typical for RP with attenuated vessels,

intraretinal pigment migration, posterior subcapsular cataract and a profound loss of both rod and cone function on electroretinography. Until the present report, no further patients have been reported with mutations in the gene.

The four patients in the present series are much younger (8-14 years) than the youngest previously reported (46 years). All affected individuals had childhood onset high myopia. Fundus examination was unremarkable in all 4 patients, but FAF imaging revealed abnormalities in the two patients imaged and OCT revealed loss of the ISe over peripheral macular areas in all patients. Electrophysiology indicated marked dysfunction in both rod and cone systems in both families. There was, however, inter-familial variation. Both siblings (patients 1 and 2) in one family showed a cone-rod dysfunction with marked macular involvement at an early age. The two siblings in the other family showed a rod>cone dysfunction with macular sparing when first examined, but subsequent recordings, in the one sibling where there was repeat testing, showed deterioration with the development of cone>rod dysfunction and severe macular involvement.

The c.1530T>A ; p.Y510* and c.3454G>T ; p.E1152* mutations identified in this study, result in transcripts shortened by 738 and 96 codons respectively. The former mutation is predicted to encode a transcript that will undergo nonsense mediated decay (NMD) and is likely to result in a complete loss of IRBP function. The second, terminal exon premature termination codon mutation is expected to avoid NMD (reviewed in [25,26]). If any protein was translated, the c.3454G>T ; p.E1152* mutation would result in a protein

lacking the putative retinol binding site of the fourth retinoid binding module and would be expected to misfold [6,11,27]. Therefore, both are predicted to be LOF alleles.

In contrast, the family identified in the earlier report had a homozygous missense mutation (p.D1080N). In vitro studies of this mutation in 293T-LC cells and the mouse cone-derived 661W cell line demonstrated that the encoded protein was misfolded and failed to be secreted[28]. The misfolded protein accumulated in the endoplasmic reticulum (ER) and induced the unfolded protein response (UPR). Interestingly, kosmotropes (chemical chaperones) and lower growth temperatures could rescue the secretion of some D1080N IRBP[28], suggesting that in vivo some of this allele might be secreted and functional. Therefore those patients are potentially hypomorphic for IRBP, as opposed to our patients whose phenotype is likely to represent the human IRBP-null phenotype. This may explain the earlier clinical presentation.

The *Irbp-/-* knockout (KO) mouse lacks expression of *Irbp* due to an intragenic deletion of all but the first 24 nucleotides of *Rbp3* exon 1[19]. The mice show photoreceptor degeneration and markedly reduced rod and cone response measured by ERG by one month of age [19,20]. There was however, only slow deterioration in rod function thereafter [20]. Furthermore, the recovery of rod function after a bleach was normal[20]. Our patients are too young for detailed psychophysical testing but it will of interest to measure the kinetics of dark adaptation at a later age to test whether human subjects show normal

recovery of function after a bleach. If the slow disease progression observed in the mouse is mirrored in the human, it raises the possibility of intervention at at stage before significant retinal degeneration.

The mechanism of photoreceptor degeneration and dysfunction in the *Irbp*-/- mouse models and our patients remains unclear. Although both rod and cone function are affected in *Irbp*-/- mice under certain conditions, such as alterations in RPE65 activity[15–18], there is no major disruption in the retinoid visual cycle, so it appears unlikely that it is these subtle changes in the visual cycle that mediate all the early changes observed in mice and patients and other mechanisms are likely to be involved. It may be the absence of IRBP from the subretinal space, where it is normally 70% of the soluble protein that leads to the physical disruption of the IPM and photoreceptor function. Alternatively, IRBP might bind other factors, such as proteins, cholesterol, vitamin E or lipids, that are essential for the maintenance of photoreceptors and it is the loss of this trophic support that underlies photoreceptor dysfunction and death. Recent studies have shown that *Irbp* KO mice have similar number of rods to wild type mice until postnatal day 15 but by postnatal day 18 there is a 20% reduction in numbers of nuclei in the ONL compared to wild type mice, followed by a spike in TUNEL-stained nuclei in the outer nuclear layer (ONL)[29]. In addition to this apoptosis-mediated cell death, receptor interacting proteins (RIP)-kinase mediated necrosis appears to be a factor in *Irbp*-/- mediated photoreceptor loss[30]. Moreover, inhibition of RIP1 with Nec1 or Nec1s prevented rod and cone photoreceptor cell death[30], highlighting potential therapeutic interventions.

Interestingly, all of the patients with the initial *RBP3* (c.3238G>A, p.D1080N) mutations were reported to be highly myopic[21]. All of our *RBP3* truncation patients are also highly myopic. In the *Irbp-/-* KO mouse, axial length is significantly increased with a corresponding severe myopic shift [29].

Collectively these data show that IRBP, which is expressed early in retinal development plays an important additional role in normal eye growth and retinal development. The reason for this is unclear, but it may relate to the role of retinoids in retinal development, or the binding of another trophic factor, as opposed to a direct effect on visual transduction. High myopia appears to be a fully penetrant phenotype associated with mutations in *RBP3* and targeted screening of this gene may be considered in patients with high myopia and retinal dystrophy.

Conclusion

This study describes the clinical phenotypes in four patients from two families with novel homozygous nonsense mutations in *RBP3* initially detected by exome sequencing. This represents only the second report of mutations in *RBP3* causing human disease. A novel phenotype is described which is associated with null *RBP3* mutations. The initial impairment of photoreceptor function with limited structural change on OCT suggests a window of opportunity for photoreceptor rescue in childhood.

Acknowledgements

The authors thank the family members for their cooperation and help in this study. We are grateful to colleagues who referred affected individuals to us at Moorfields Eye Hospital and to those who contributed to the assembly of the early onset retinal dystrophy database, particularly Panos Sergouniotis, Alice Davidson, Alan Bird, Michel Michaelides, Genevieve Wright, Sophie Devery, Ravinder Chana, Beverley Scott, and Naushin Waseem. Additionally, we thank the UCL-exome consortium for access to control data.

Supported by grants from The National Institute for Health Research and Biomedical Research Centre at Moorfields Eye Hospital and the UCL Institute of Ophthalmology (London, UK), The Foundation Fighting Blindness (Owings Mills, MD, USA), Fight For Sight (London, UK), Moorfields Eye Hospital Special Trustees (London, UK) and Rosetrees Trust (Edgware, UK).

References

1. Chen S, Wang Q-L, Nie Z, et al. Crx, a Novel Otx-like Paired-Homeodomain Protein, Binds to and Transactivates Photoreceptor Cell-Specific Genes. *Neuron*. 1997;19(5):1017-1030.

2. Fei Y, Matragoon S, Smith SB, et al. Functional dissection of the promoter of the interphotoreceptor retinoid-binding protein gene: the cone-rod-homeobox element is essential for photoreceptor-specific expression in vivo. *J Biochem*. 1999;125(6):1189-99.

3. Liou GI, Bridges CD, Fong SL, Alvarez RA, Gonzalez-Fernandez F. Vitamin A transport between retina and pigment epithelium--an interstitial protein carrying endogenous retinol (interstitial retinol-binding protein). *Vision Res*. 1982;22:1457-1467.

4. Fong SL, Liou GI, Landers RA, et al. Characterization, localization, and biosynthesis of an interstitial retinol-binding glycoprotein in the human eye. *J Neurochem*. 1984;42:1667-1676.

5. Redmond TM, Wiggert B, Robey FA, et al. Isolation and characterization of monkey interphotoreceptor retinoid-binding protein, a unique extracellular matrix component of the retina. *Biochemistry*. 1985;24:787-793.

6. Loew A, Gonzalez-Fernandez F. Crystal structure of the functional unit of interphotoreceptor retinoid binding protein. *Structure*. 2002;10:43-49.

7. Ghosh D, Griswold JB, Bevilacqua T, Gonzalez-Fernandez F. Purification of the full-length Xenopus interphotoreceptor retinoid binding protein and growth of diffraction-quality crystals. *Mol Vis*. 2007;13:2275-81.

8. Carlson A, Bok D. Promotion of the release of 11-cis-retinal from cultured retinal pigment epithelium by interphotoreceptor retinoid-binding protein. *Biochemistry*. 1992;31(37):9056-62.

9. Edwards RB, Adler AJ. IRBP enhances removal of 11- cis - retinaldehyde from isolated RPE membranes. *Exp Eye Res*. 2000;70(2):235-45.

10. Gonzalez-Fernandez F. Interphotoreceptor retinoid-binding protein - An old gene for new eyes. *Vision Res*. 2003;43:3021-3036.

11. Gonzalez-fernandez F, Ghosh D. Focus on Molecules : Interphotoreceptor retinoid-binding protein (IRBP). *Exp Eye Res*. 2008;86:169-170.

12. Crouch RK, Hazard ES, Lind T, Wiggert B, Chader G, Corson DW. Interphotoreceptor retinoid-binding protein and alpha-tocopherol preserve the isomeric and oxidation state of retinol. *Photochem Photobiol*. 1992;56(2):251-5.

13. Palczewski K, Van Hooser JP, Garwin GG, Chen J, Liou GI, Saari JC. Kinetics of visual pigment regeneration in excised mouse eyes and in mice with a targeted disruption of the gene encoding interphotoreceptor retinoid-binding protein or arrestin. *Biochemistry*. 1999;38:12012-12019.

14. Saari JC. Vitamin A metabolism in rod and cone visual cycles. *Annu Rev Nutr*. 2012;32:125-45.

15. Jin M, Li S, Nusinowitz S, et al. The role of interphotoreceptor retinoid-binding protein on the translocation of visual retinoids and function of cone photoreceptors. *J Neurosci*. 2009;29(5):1486-95.

16. Parker RO, Fan J, Nickerson JM, Liou GI, Crouch RK. Normal cone function requires the interphotoreceptor retinoid binding protein. *J Neurosci*. 2009;29(14):4616-21.

17. Parker R, Wang J-S, Kefalov VJ, Crouch RK. Interphotoreceptor retinoid-binding protein as the physiologically relevant carrier of 11-cis-retinol in the cone visual cycle. *J Neurosci*. 2011;31(12):4714-9.

18. Kolesnikov A V, Tang PH, Parker RO, Crouch RK, Kefalov VJ. The mammalian cone visual cycle promotes rapid M/L-cone pigment regeneration independently of the interphotoreceptor retinoid-binding protein. *J Neurosci*. 2011;31:7900-7909.

19. Liou GI, Fei Y, Peachey NS, et al. Early onset photoreceptor abnormalities induced by targeted disruption of the interphotoreceptor retinoid-binding protein gene. *J Neurosci*. 1998;18:4511-4520.

20. Ripps H, Peachey NS, Xu X, Nozell SE, Smith SB, Liou GI. The rhodopsin cycle is preserved in IRBP “knockout” mice despite abnormalities in retinal structure and function. *Vis Neurosci*. 2000;17(1):97-105.

21. Den Hollander AI, McGee TL, Ziviello C, et al. A homozygous missense mutation in the IRBP gene (RBP3) associated with autosomal recessive retinitis pigmentosa. *Invest Ophthalmol Vis Sci*. 2009;50(4):1864-72.

22. Bach M, Brigell MG, Hawlina M, et al. ISCEV standard for clinical pattern electroretinography (PERG): 2012 update. *Doc Ophthalmol*. 2013;126(1):1-7.

23. Marmor MF, Fulton AB, Holder GE, et al. ISCEV Standard for full-field clinical electroretinography (2008 update). *Doc Ophthalmol*. 2009;118(1):69-77.

24. Abecasis GR, Auton A, Brooks LD, et al. An integrated map of genetic variation from 1,092 human genomes. *Nature*. 2012;491(7422):56-65.

25. Schweingruber C, Rufener SC, Zünd D, Yamashita A, Mühlemann O. Nonsense-mediated mRNA decay - mechanisms of substrate mRNA recognition and degradation in mammalian cells. *Biochim Biophys Acta*. 2013;1829(6-7):612-23.

26. Brogna S, Wen J. Nonsense-mediated mRNA decay (NMD) mechanisms. *Nat Struct Mol Biol*. 2013;16(2):107-13.

27. Gonzalez-Fernandez F, Baer CA, Ghosh D. Module structure of interphotoreceptor retinoid-binding protein (IRBP) may provide bases for its complex role in the visual cycle - structure/function study of Xenopus IRBP. *BMC Biochem*. 2007;8:15.

28. Li S, Yang Z, Hu J, et al. Secretory defect and cytotoxicity: the potential disease mechanisms for the retinitis pigmentosa (RP)-associated interphotoreceptor retinoid-binding protein (IRBP). *J Biol Chem*. 2013;288(16):11395-406.

29. Wisard J, Faulkner A, Chrenek MA, et al. Exaggerated eye growth in IRBP-deficient mice in early development. *Invest Ophthalmol Vis Sci*. 2011;52(8):5804-11.

30. Sato K, Li S, Gordon WC, et al. Receptor interacting protein kinase-mediated necrosis contributes to cone and rod photoreceptor degeneration in the retina lacking interphotoreceptor retinoid-binding protein. *J Neurosci*. 2013;33(44):17458-68.

Figure legends

Figure 1: Pedigrees of 2 families with mutation segregation

Figure 2: Full-field and pattern ERGs (PERG) in patients 1 (age 10 years), 2 (age 9 years),3 (age 5 years) and 4 (age 7 years) and a normal control. No significant inter-ocular asymmetries were present and data are shown for one eye only. Dark-adapted ERGs are shown for white flash strengths of 0.01 (DA 0.01) and 10.0 cd.s.m^{-2} (DA 10.0); Light-adapted ERGs use a 3.0 cd.s.m^{-2}

flash strength at 30Hz (LA 30Hz) and 2Hz (LA 3.0). ERGs in case 4 have a 20ms pre-stimulus delay, other than the 30Hz response. Broken lines replace blink artefacts. All patients have delayed and subnormal cone flicker ERGs in keeping with generalized cone system dysfunction. There is also marked rod photoreceptor dysfunction as shown by the subnormal DA 10.0 a-wave amplitude and subnormal DA 0.01 ERGs, with patient 4 being particularly severely affected. The loss of PERG in patients 1 and 2 indicates severe macular involvement; there is macular sparing in case 3 and relative sparing in case 4. See text for further details.

Figure 3: Retinal imaging: 1a-d patient 2 left eye, (1a) color fundus photograph montage from 30 degree photographs, demonstrating a tessellated, myopic fundus only (1b) 55 degree fundus autofluorescence (FAF) imaging with a patchy ring of increased autofluorescence in the region of the vascular arcades, (1c) optical coherence tomography (OCT) scan through the central macula, no abnormalities found (1d) OCT scan of superior macula with disrupted inner segment ellipsoid (ISe) band, and absent ISe band nasal to arrow; 2a-d patient 4 right eye, (2a) 35 degree color fundus photograph of posterior pole, no abnormalities found (2b) 30 degree FAF imaging with multiple foci of reduced autofluorescence, (2c) OCT scan through the central macula, no abnormalities found (2d) OCT scan of superior macula with disrupted ISe band, and absent ISe band nasal to arrow.
Key: RPE, retinal pigment epithelium; DS, dioptre sphere

Patient Family (gender)	Mutation details	Ages of review	Fundus	Age at last electrophysiology, key findings	Latest visual acuity, logMAR (Snellen equivalent)	Latest refractive error	Strabismus
1 GC17452 (m)	c.3454G>T ; p.E1152*	5-13 years	Myopic changes	10 years; cone>rod dysfunction with marked macular involvement	R 0.44 (20/50) L 0.42 (20/50)	R -23.00/-2.50 x 100 L -23.00/-2.50 x 170	Slight exophoria
2 GC17452 (f)		4-12 years	Myopic changes	9 years; as above but more marked rod system involvement	R 0.26 (20/40) L 0.26 (20/40)	R -12.50/-2.00 x 20 L -1.00/-1.75 x 170	Small left convergent squint, Left strabismic amblyopia treated with patching
3 GC19774 (m)	c.1530T>A ; p.Y510*	2-14 years	Myopic changes	13 years; marked deterioration into cone>rod dysfunction with macular involvement; at age 5 years there was a rod>cone abnormality with macular sparing	R 0.12 (20/25) L 0.02 (20/20)	R -12.25/-1.00 x 50 L -13.00/-2.00 x 140	Small exophoria
4 GC19774 (m)		2-8 years	Myopic changes	7 years, rod>cone abnormality with relative macular sparing	R 0.42 (20/50) L 0.44 (20/50)	R -6.25/-1.25 x 180 L -6.75/-1.00 x 5	Small left/alternating esotropia

Table 1: Clinical summary.

	Number of variants
Total	>100,000
Post quality filtering, exonic ± 5 nucleotides	25,799
Variants with MAF <0.001 in control datasets*	623
Homozygous	27
Loss of function	2

*UCL-exomes dataset and ESP database

Table 2: WES variant filtering strategy

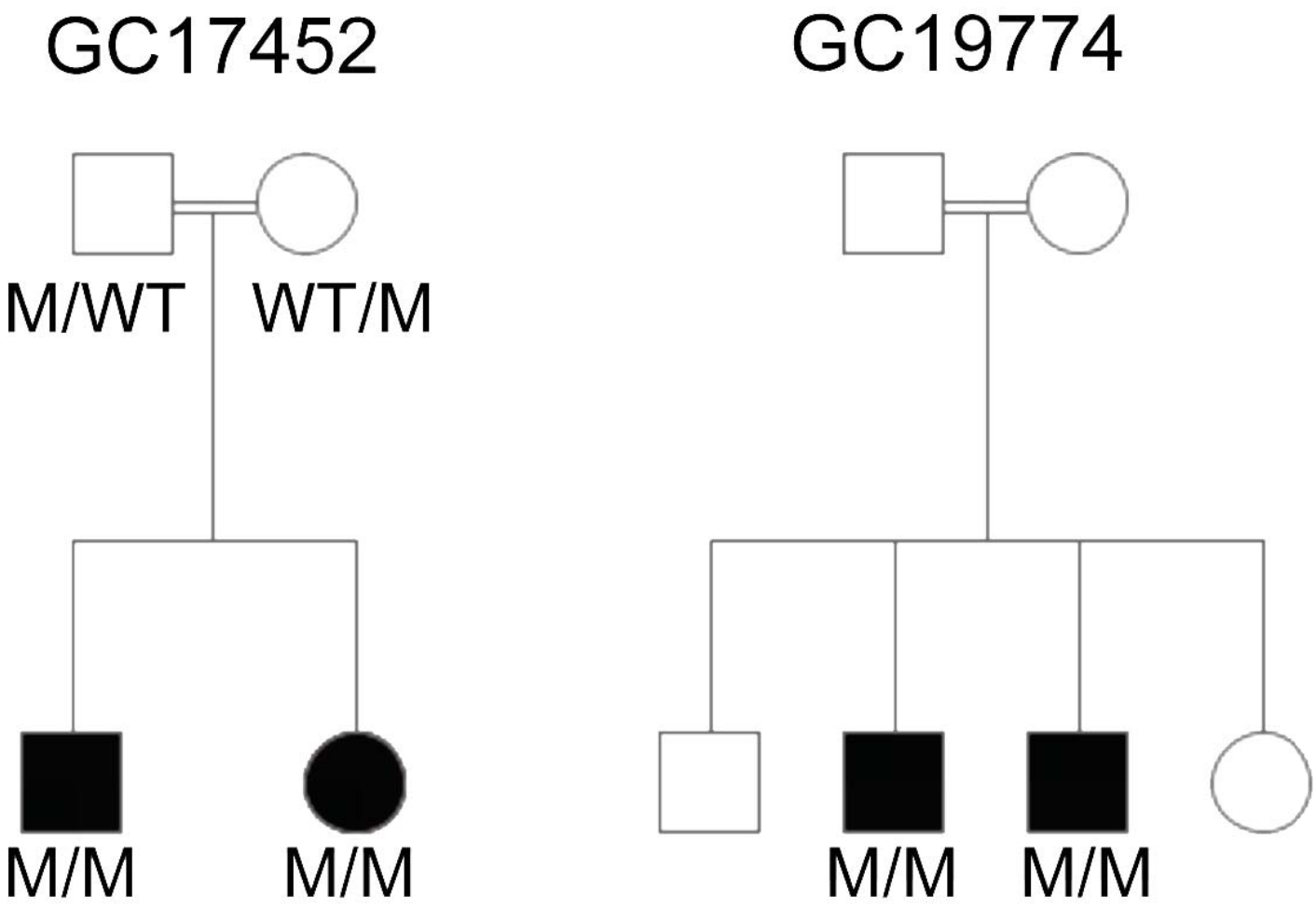
GC17452
M/WT
WT/M
M/M
M/M
GC19774
M/M
M/M

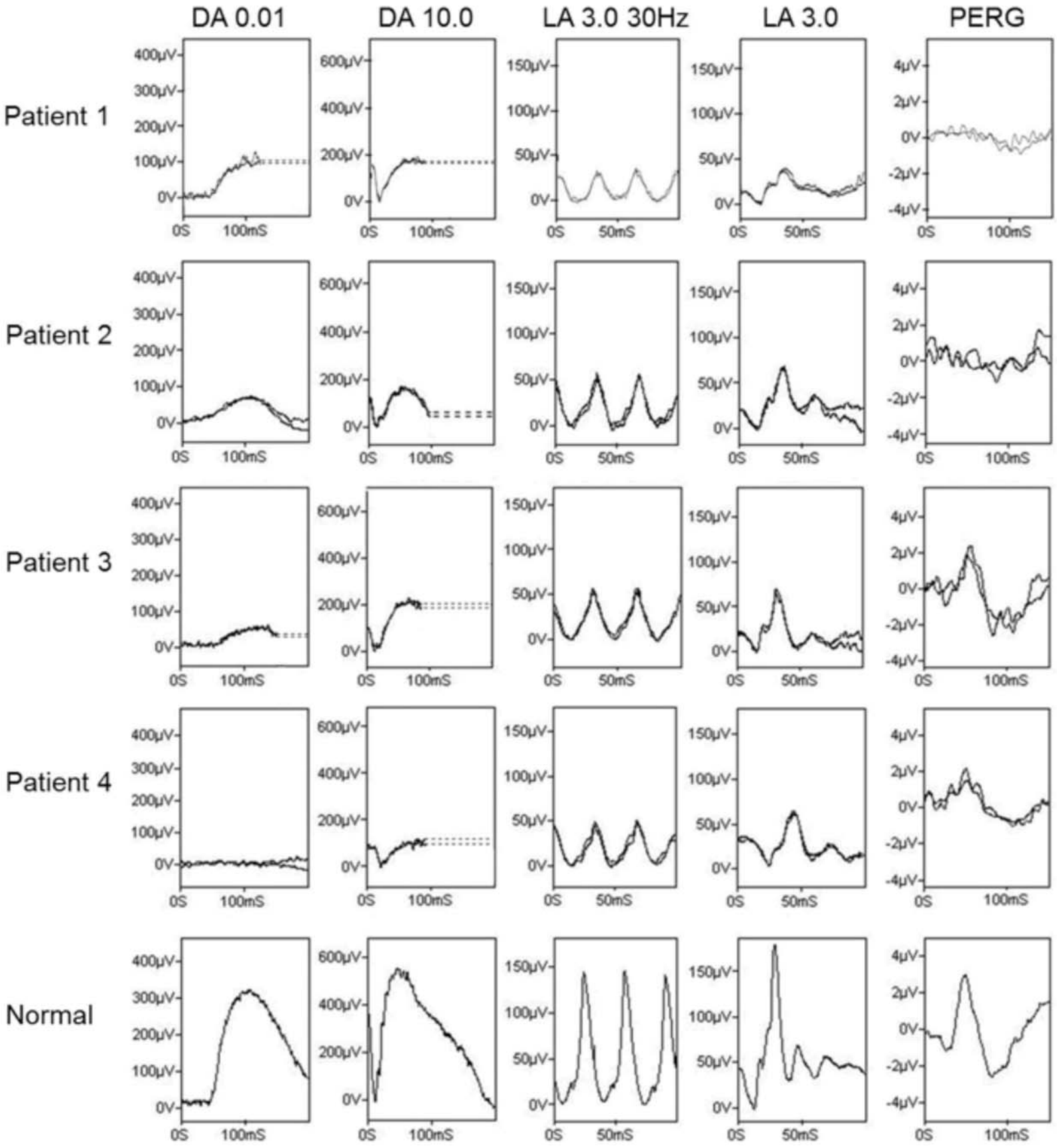
DA 0.01
DA 10.0
LA 3.0 30Hz
LA 3.0
PERG
Patient 1
Patient 2
Patient 3
Patient 4
Normal
400µV
300µV
200µV
100µV
0V
600µV
150µV
50µV
4µV
2µV
-2µV
-4µV
0S
100mS
50mS

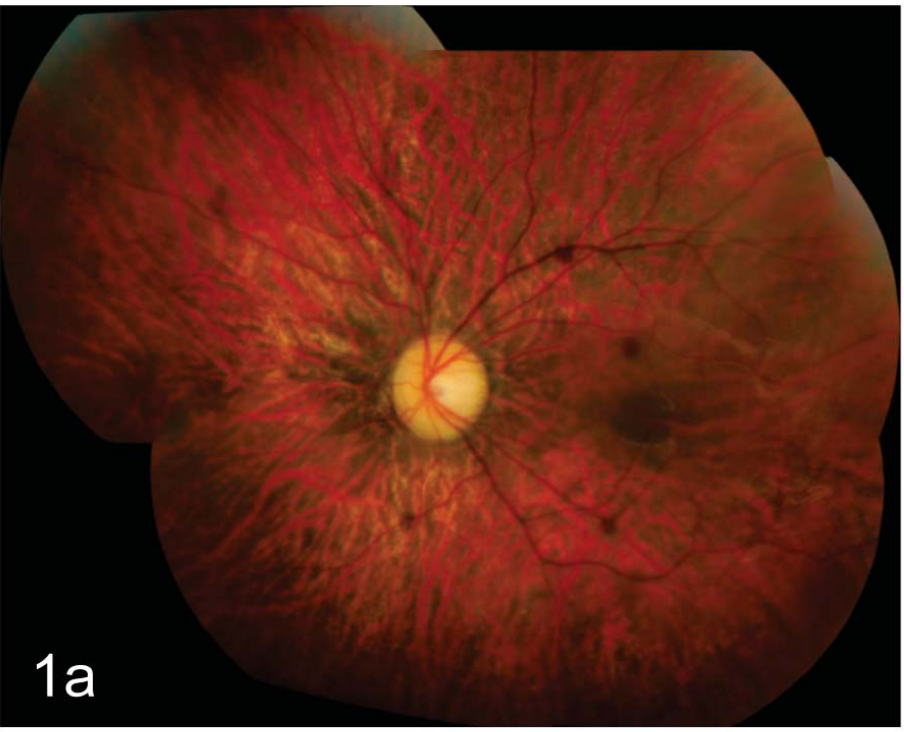
1a

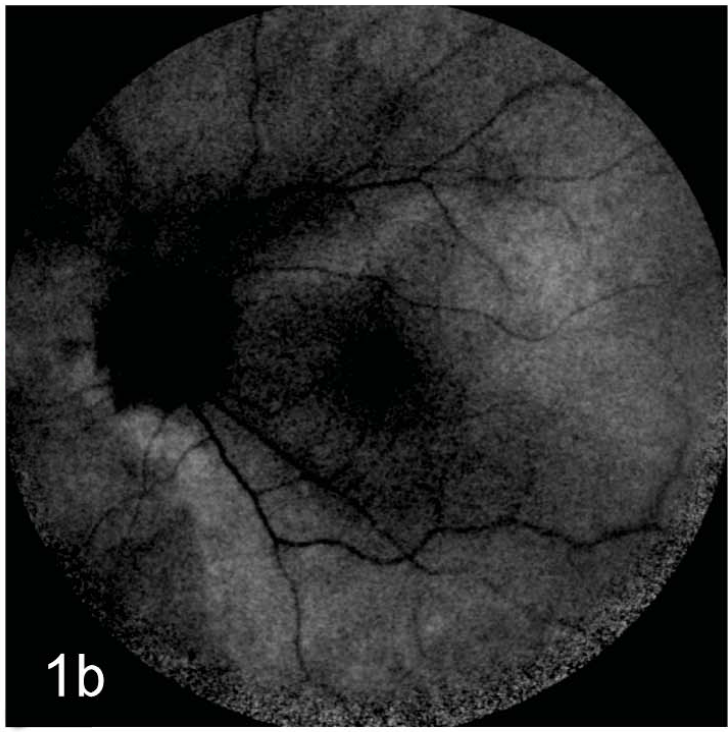
1b

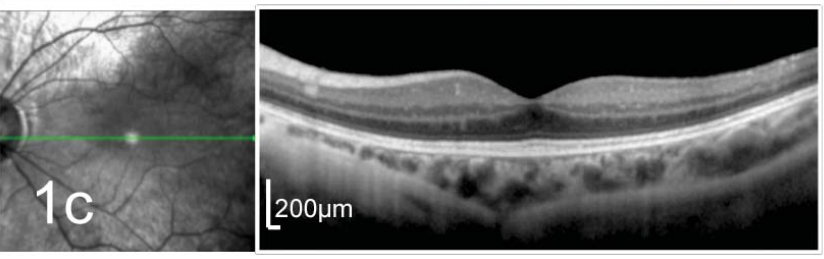
1c
200µm

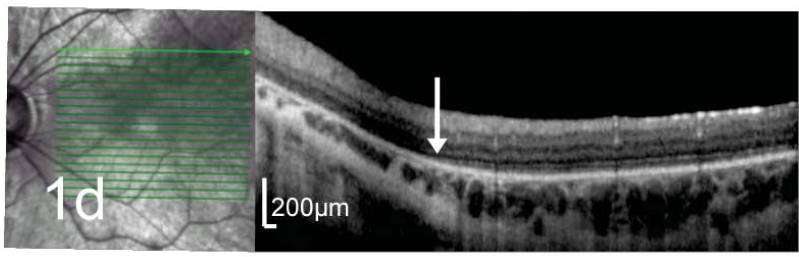
1d
200µm

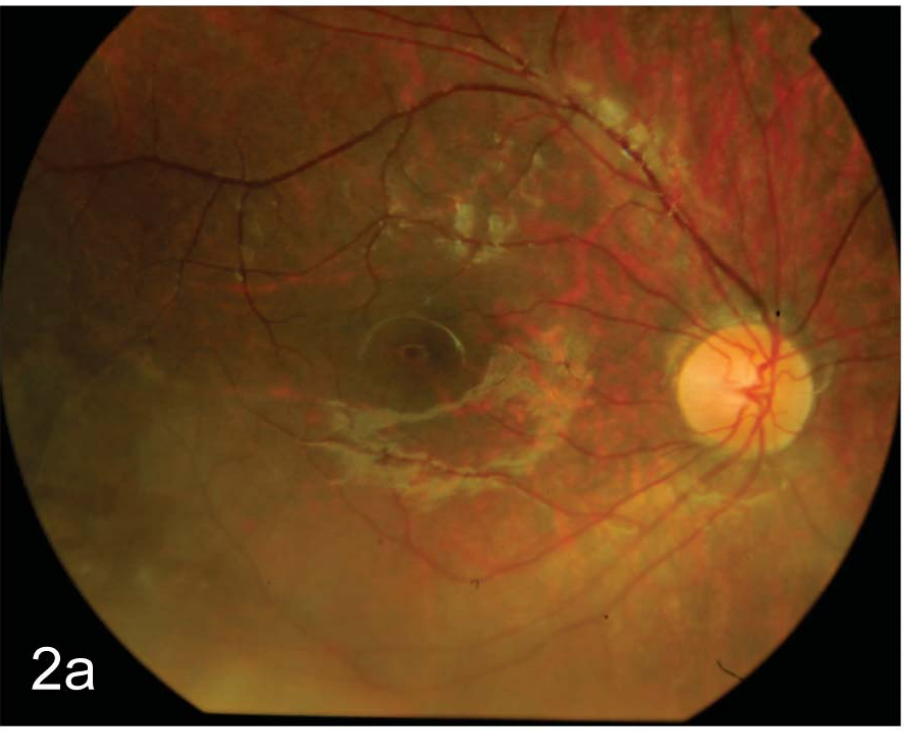
2a

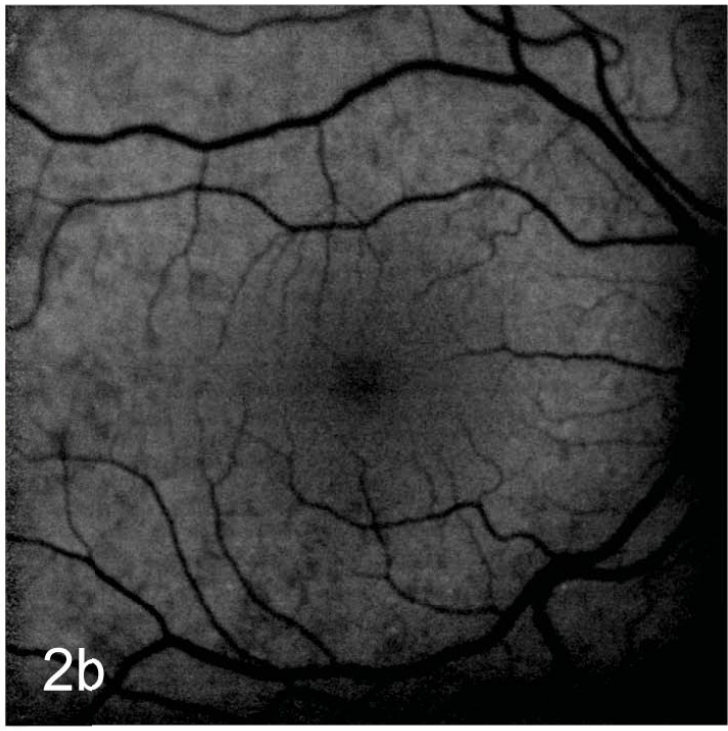
2b

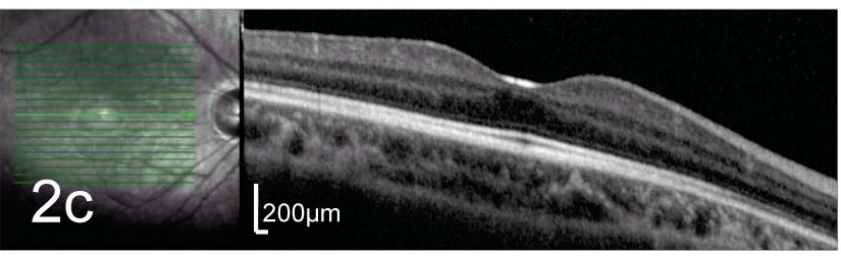
2c
200µm

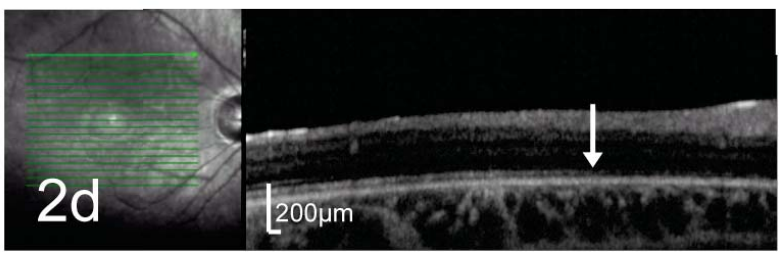
2d
200µm